

A Bandpass filter-bank model of auditory sensitivity in the humpback whale

Dorian S. Houser¹, David A. Helweg^{2*} and Patrick W. B. Moore³

¹National Research Council Associate, SPAWARSYSCEN-San Diego, San Diego, CA 92152, USA

²Code 3501E, SPAWARSYSCEN-San Diego, San Diego, CA 92152, USA

³Code 3501B, SPAWARSYSCEN-San Diego, San Diego, CA 92152, USA

Abstract

Concerns that water-borne, anthropogenic sound could negatively impact whale species continue to escalate. Unfortunately, the auditory sensitivity of mysticete whales is unknown, impeding assessment of underwater sound exposure on these animals. In light of this problem, a mathematical function describing frequency sensitivity by position along the relative length of the basilar membrane of a humpback whale (*Megaptera novaeangliae*) was integrated with known data on the cat and human to predict the audiogram for the humpback whale. The predicted audiogram was the typical mammalian U-shape and indicated sensitivity to frequencies from 700 Hz–10 kHz, with maximum relative sensitivity (values approaching 0) between 2–6 kHz. A model of humpback hearing subsequently was created as a series of pseudo-Gaussian bandpass filters. Sensitivity of the model was optimized to the predicted audiogram via meta-evolutionary programming (EP). The number, frequency distribution, and shape of the filters in the model were evolved with the EP and the sensitivity of the model evaluated through a simulated hearing test. Maximum deviations between model sensitivity and predicted humpback sensitivity never exceeded ten percent. Through an integrated approach, the first predicted humpback audiogram was made and used to develop the first bandpass model of the humpback ear.

Key words: audiogram, evolutionary program, filter model, hearing, humpback whale, anthropogenic sound

Introduction

A substantial increase in anthropogenic noise in the marine environment has occurred over the last century as a result of increased scientific exploration, shipping traffic, geophysical and oil industry

activities, and military operations. For many marine species that are sensitive to acoustic signals or reliant on them for communication, foraging, reproduction, or navigation, the impact of exposure to such sounds is unknown. Anthropogenic noise can potentially interfere with the production or reception of these signals through masking, behavioral disturbances, temporary threshold shifts, or permanent damage to the auditory system (Richardson & Würsig, 1997). Of primary concern are mysticete whales (baleen whales) whose sounds range from 15 Hz–8000 Hz, suggesting auditory sensitivity to frequencies commonly generated by anthropogenic sources (Clark, 1990; Herman & Tavolga, 1980; Richardson & Würsig, 1997). Assessment of such impacts to date has been limited to observations of mysticete responses to industrial sound exposure and playbacks of anthropogenic signals (Frankel & Clark, 1998; Malme *et al.*, 1985; Malme *et al.*, 1988; Maybaum, 1989; Richardson *et al.*, 1990; Richardson *et al.*, 1985). Unfortunately, interpretation of experimental results has been confounded by the intra- and inter-specific variability in observed behavior and, in some instances, an apparent lack of correlation between whale behavior and received sound level.

Mysticetes are too large to maintain in a controlled environment necessary for effective traditional audiometric assessment. Psychophysical and physiological studies of cetacean (baleen and toothed whales) hearing have been restricted to the smaller odontocetes (toothed whales), with the bottlenose dolphin (*Tursiops truncatus*) being the species studied most (Au, 1993; Au & Moore, 1990; Busnel & Fish, 1979; Herman & Arbeit, 1972; Johnson, 1968a, 1968b; Nachtigall & Moore, 1988; Popov *et al.*, 1996; Popov *et al.*, 1997; Supin *et al.*, 1993). Using psychophysical measures of dolphin hearing and the anatomy of the dolphin auditory system, Roitblat and colleagues (1993) constructed a model of the dolphin ear as a series of overlapping frequency-domain filters. Sensitivity to acoustic

signals above 50 kHz was comparable to that observed in the dolphin and was later improved across the full range of dolphin hearing through the application of evolutionary programming (EP) (Houser *et al.*, 2001), an optimization technique that emulates natural evolutionary processes. Extending these types of models to mysticete audition is a logical step towards predicting mysticete sensitivity to anthropogenic sounds, particularly since more direct psychophysical and physiological procedures are not likely in the immediate future.

It can be argued that mysticetes have a conventional mammalian ear adapted to low frequency reception due to the presence of a voluminous middle ear cavity and the loose coupling of the ossicles (Ketten, 1997). Furthermore, the anatomy and biomechanical properties of the basilar membrane can be used to predict frequencies to which terrestrial mammals are sensitive (Greenwood, 1990), and this approach has been extended and modified to predict frequencies to which whales are sensitive (Ketten, 1994; Ketten & Wartzok, 1990; Norris, 1981). If it is assumed that mysticetes have a conventional mammalian ear, and a cochlear frequency-position function can be determined from the cochlear anatomy, then psychoacoustic and anatomical measures of hearing from a terrestrial mammal with a conventional ear can be used to create a predictive mysticete auditory threshold function. A bandpass ear-filter model can then be constructed and output optimized to the predicted threshold as has been performed for the bottlenose dolphin (Houser *et al.*, 2001; Roitblat *et al.*, 1993).

The objective of this study was to create a mathematical model of a mysticete ear, specifically that of the humpback whale (*Megaptera novaeangliae*). Anatomical indices of hearing were derived for the humpback from histological measurements of the basilar membrane and related structures (Ketten, in preparation), thus providing the cochlear frequency-position function necessary for model development. In the first part of the study, we generated a predicted audiogram for the humpback whale. In the second part of the study, evolutionary programming techniques were used to create a bandpass-filter model with output that matched the predicted humpback whale audiogram.

Materials and Methods

Predicting the humpback whale audiogram

Since empirical auditory threshold measurements for the humpback do not exist, an audiometric function predicting the frequency-dependent relative sensitivity was created on the assumption that the humpback ear could be modeled as a conventional mammalian ear. This task involved integrating the auditory threshold function and

frequency-position function of two well-studied terrestrial mammals, the cat and human, and mapping the resulting sensitivity-position functions onto the frequency-position map of the humpback whale ear.

A basilar membrane frequency-position function was determined from morphometric analyses of extracted humpback whale basilar membranes. The method for determining the frequency response of the basilar membrane by position along its length is the subject of an upcoming paper and the methodological details are not presented here (Ketten, in preparation; but see Ketten, 1993, and Ketten, 1994, for summaries of previous modeling effort). Ten estimates of frequency by position along the basilar membrane were supplied from these analyses (D. Ketten, personal communication) and the distribution of frequencies along the relative length of the basilar membrane fit with a 3rd order exponential function (Figure 1, $r^2=0.99$). The exponential function, thus became the frequency-position function for the humpback basilar membrane.

Auditory thresholds and cochlear frequency-position functions of the cat and human were integrated with the humpback frequency-position function to create an audiogram for the humpback whale. The goal of this procedure was to generate an audiometric function generally in agreement with other observed mammalian thresholds. Scaled threshold values were combined so that any auditory specialization would be averaged out to some degree. This procedure does not imply that either the cat or human audiogram is more similar to the audiogram of the humpback whale than are other mammalian species. They are simply two species with conventional mammalian ears. Other species with generalist audiograms could have been utilized.

Cochlear frequency-position functions were obtained for the human (Greenwood, 1990) and cat (Lieberman, 1982) and adjusted such that exponential coefficients accommodated the expression of basilar membrane length in proportional units. Thus, for the human:

$$f(x)=165.4(10^{2.1x}-1) \quad (1)$$

and for the cat:

$$f(x)=456(10^{2.1x}-0.8) \quad (2)$$

where, $f(x)$ is frequency and x is a proportion of basilar membrane length. For all frequencies at which hearing thresholds have been tested in the human and cat, as reported by Fay (1988), the respective relative position on the basilar membrane was determined. Relative position determinations for the cat were limited to frequencies between

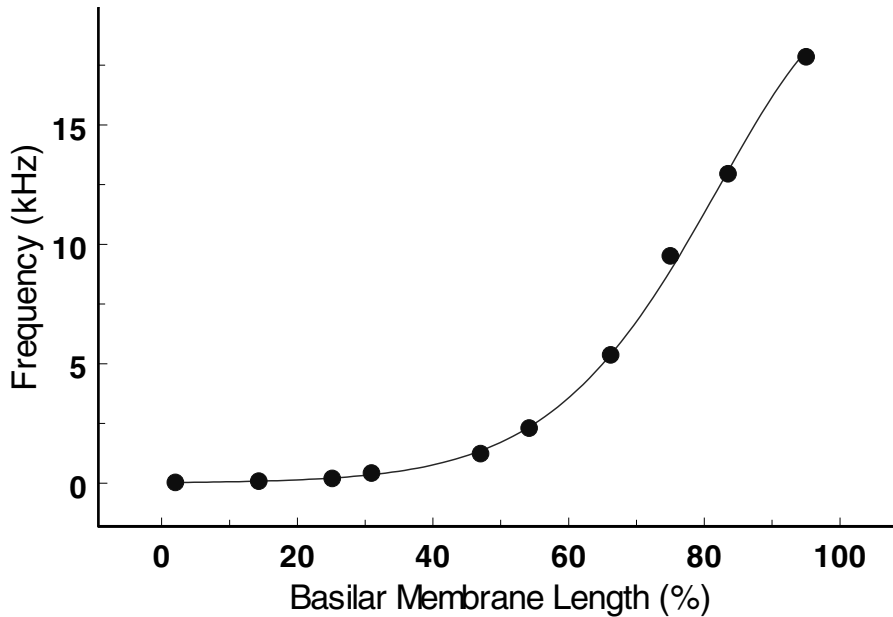


Figure 1. Frequency plotted against relative position on the basilar membrane for the humpback whale (data provided by D. Ketten). A 3rd order exponential function was fit to the data ($y=0.08*\exp(0.15x - (8.74e-4)x^2 + (1.63e-6)x^3)$) to create the frequency-position function.

100 Hz and 60 kHz since this was the frequency range covered by the experimentally determined basilar membrane frequency-position function (Lieberman, 1982). Frequencies from 64 Hz–18,780 Hz, reported in Fay (1988) for adult human auditory thresholds, fell within the experimentally determined frequency-position function of the human basilar membrane (Greenwood, 1990).

Frequency-dependent threshold intensities (W/cm^2) of the cat and human were plotted as a function of relative basilar membrane position. Threshold intensities were converted to dB re: minimum intensity and fit with a 4th order polynomial (Figure 2, $r^2=0.66$). This intensity-position function was integrated with the humpback cochlear frequency-position function to produce an audiogram for the humpback. Thresholds were subsequently scaled from zero to one.

Optimized filter-bank ear model design

Development of a computational ear model, similar to that described by Houser and colleagues (2001) for the dolphin, relies on the existence of a target threshold function to which sensitivity can be optimized. To create a computational ear model, the predicted humpback whale audiogram (Figure 3) was used as the target threshold function. Relative threshold values for frequencies used in ear model development, that were not explicitly defined by the

humpback audiogram, were determined via cubic spline interpolation.

Ear models were created as a series of overlapping bandpass filters with a pseudo-Gaussian (PG) shape, as described for the bottlenose dolphin (Houser *et al.*, 2001). Filter shapes were 'pseudo-Gaussian' in that the standard deviation (σ) was removed from the denominator of the distribution equation to control variations in filter amplitude that accompany changes in σ . These were not digital IIR or FIR filters; instead, the Gaussian shape delimited the bandpass region in the spectral power domain. Pseudo-Gaussian filter shapes were generated with peak sensitivity corresponding to the center frequency (μ) of the filter, according to:

$$\frac{1}{\sqrt{2\pi}} \exp\left(-\frac{1}{2}\left(\frac{x_i - \mu}{\sigma}\right)^2\right) \quad (3)$$

where, x_i is the i^{th} point on the distribution curve. Each filter was described by a 256 bin vector with each bin corresponding to a 100 Hz width such that the frequency range covered by the filter shape was ~ 0.1 –25.6 kHz.

Filter center frequencies were distributed from 100 Hz to 18 kHz. Restriction of filter center frequency to a maximum of 18 kHz was performed to minimize sensitivity above 18 kHz, a characteristic

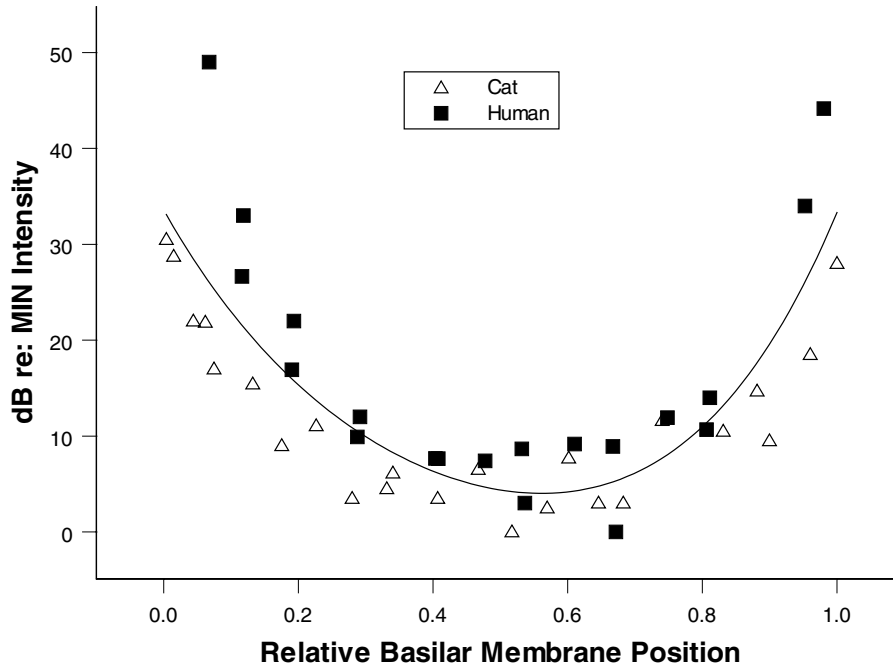


Figure 2. Relative hearing sensitivity of the cat and human as a function of relative basilar membrane length. The relationship was determined by integrating experimentally derived frequency-position functions (Greenwood, 1990; Liberman, 1982) for each species with their respective averaged frequency-dependent thresholds (obtained from Fay, 1988). The fitted function ($y=3.36 - 12.4*x + 19.72*x^2 - 19.1*x^3 + 11.75*x^4$) provides a predictive sensitivity-position function.

of the predicted humpback audiogram. Filter center frequency (μ) was calculated as a fractional power of the frequency range emulating the non-uniform spacing of characteristic frequencies on the basilar membrane (Geisler & Cai, 1996). The equation was:

$$\mu = 180 \frac{f_j}{F_n} \quad (4)$$

where, F_n is defined as the total number of filters used in the model, f_j was the j^{th} filter, and the constant 180 was used to describe the predicted range of hearing (i.e., $180 \times 100 \text{ Hz binwidth} = 18 \text{ kHz}$).

Variation in filter shape was achieved by implementing a frequency-dependent amplitude-scaling factor (S) and 3-dB bandwidth (Q_3) function for each filter. Q_3 was determined as an exponential function of filter center frequency so that bandwidth ranged from constant-Q to a curvilinear variation with center frequency. It was defined as the ratio of μ to the bandwidth at 3 dB below the peak amplitude of the filter in the spectral power domain. The relationship between σ and Q_3 was derived from the PG equation as:

$$\sigma = \frac{\mu}{\alpha Q_3} \quad (5)$$

where, $\alpha=2.351$. The value of α was empirically determined in the power domain by systematically varying μ and Q_3 and observing the relationship to σ . Amplitude scaling was determined using a frequency-dependent function that could create a bank of filters, ranging from equal gain to a bank of filters with variable gain. The scaling factor, S , was determined as a base value to a negative fractional power derived from sequential filter position within the frequency range such that:

$$S = y^{\left(\frac{f_j}{F_n} - 1\right)} \quad (6)$$

where, y is an evolved base value. This factor is analogous to the scaling used by Roitblat *et al.* (1993), which was based upon hair cell densities along the basilar membrane. The scaling factor was loosely defined in this model implementation so that the evolutionary program would not be constrained in its search for a suitable model structure. Substitution of parameters into the

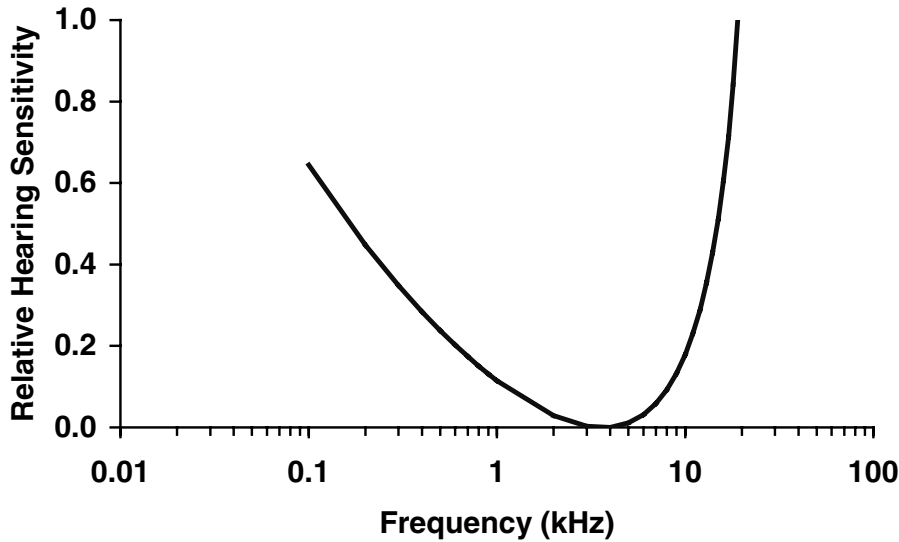


Figure 3. Relative hearing sensitivity function created by scaling humpback frequency-dependent sensitivities from 0–1. Prior to scaling, frequency-dependent sensitivities were determined by integrating the humpback frequency-position function (Figure 1) with the sensitivity-position function derived from cat and human audiometric and anatomic data (Figure 2).

pseudo-Gaussian equation thus produced the filter form function:

$$\frac{S}{\sqrt{2\pi}} \exp^{-\frac{1}{2} \left(\left(x_i - (180) \frac{f_i}{F_n} \right) / \left(\frac{180 F_n}{2.351 Q_s} \right) \right)^2} \quad (7)$$

The filter bank model assumes that, since model design is optimized to threshold conditions, the transfer functions of the outer and middle ear are translated, and therefore reflected, in basilar membrane motion at levels of threshold exposure. This static condition does not require that middle and outer ear transfer functions be addressed, they are implied in the model and reflected in the filter design. Furthermore, transfer functions for the middle and outer ear have yet to be defined for the humpback whale, obviating their inclusion in the model.

Evolutionary programming (EP)

Parameters determining filter shape and distribution were submitted to an EP scheme with self-adaptive mutation (Fogel, 1995) and a Cauchy mutation operator (Chellapilla & Fogel, 1997). Through an iterative process of parameter cloning, parameter mutation, and model evaluation the EP optimized the sensitivity of populations of encoded ear models to that of the predicted humpback audiogram. The EP used 20 'parent' parameter sets with 20 'offspring' produced per generation, a form of evolutionary algorithm (EA) commonly known

as a (20+20) – EA (Schwefel, 1981). The reader is referred to Houser *et al.* (2001) for a thorough description of the EP process and its application to biomimetic filter design.

Parameters of the evolutionary program are given in Table 1, which lists respective random initialization boundaries and the initial standard deviation used in calculating mutation step-size. Parameters including the base value (γ) of the amplitude scaling factor (S) and the equation determining Q_s were mutated via a Cauchy random variable (Chellapilla & Fogel, 1997). The total number of filters (F_n) was mutated in a probabilistic manner such that there was an equal probability that F_n would increase by 1 or 2, decrease by 1 or 2, or stay the same, if $20 < F_n < 400$. If $F_n \leq 20$, there was an equal probability that F_n would increment by 1, 2, or stay the same. Conversely, if $F_n \geq 400$, there was an equal probability that F_n would decrement by 1, 2, or remain the same. Thus, minimum and maximum possible values of F_n were 19 and 401, respectively.

Following each generation of the evolutionary program, defined by parameter cloning and mutation, sets of parameter values were inserted into the filter function described in Equation 7 to create a bank of filters. Each filter bank was evaluated for its sensitivity through a simulated audiometric assessment at {0.1, 0.2, 0.3, . . . , 0.9} and {1.0, 2.0, 3.0, . . . , 19.0} kHz, for a total of 28 comparison frequencies. This was achieved by first creating a library of noise (N) and signal+noise (S+N) trials

Table 1. Model parameter values with initialization limits, initial standard deviations, and description of parameter function.

Parameter	Minimum initialization limit	Maximum initialization limit	Initial standard deviation
y	0	10	0.5
m	0	10	0.5
b	0	2	0.15
x	0	0.025	0.001
F_n	(b)	(b)	(c)

Definition (a)	
y	base value for filter amplitude scaling (used to calculate S)
m	slope of the equation determining Q_3
b	intercept of the equation determining Q_3
x	coefficient of the exponent in the equation determining Q_3
F_n	filter number

(a) See Houser *et al.* (2001) for details on the equations determining S and Q_3 .

(b) Filter number explicitly set to 40.

(c) Probabilistic mutation limited to integer step sizes of ± 2 .

with which to test the sensitivity of the filters. Each library consisted of a 5000×256 matrix with row elements corresponding to a binwidth of ~ 100 Hz, i.e. equivalent to the frequency distribution described for the filter arrays. To simulate noise, bins were initialized with randomly generated values ranging from 0.00 to 0.25. In the S+N library, a real valued 'signal' of 0.55 was added to the bin corresponding to a given frequency. For instance, to add a signal to the 1 kHz frequency of the S+N library, 0.55 was added to the value of the 10th bin of each row of the library. This matrix thus became the 1 kHz S+N library, or (S_1+N).

The response of the filters to N trials (\mathbf{R}_N) and S_f+N trials (\mathbf{R}_{S_f+N}) was derived by multiplying the filter matrix by the rows of the N library, and rows of the S_f+N library, respectively, for a given test frequency such that:

$$\mathbf{R}_N(i) = \mathbf{F} * \mathbf{N}(i), \quad i = 1, 2, 3, \dots, 5000 \quad (8)$$

$$\mathbf{R}_{S_f+N}(i) = \mathbf{F} * \mathbf{SN}_f(i), \quad i = 1, 2, 3, \dots, 5000 \quad (9)$$

where, \mathbf{N} and \mathbf{SN}_f represent the row vectors of the N library and the (S_f+N) library at frequency f . A squared-difference (\mathbf{SD}) vector was then determined as:

$$\mathbf{SD}_{(i)} = [\mathbf{R}_{S_f+N}(i) - \mathbf{R}_N(i)]^2, \quad i = 1, 2, 3, \dots, 5000 \quad (10)$$

and the sensitivity metric (ϕ_f) for the tested frequency determined as:

$$\phi_f = 0.0002 \sum_i^{5000} \sqrt{\sum_j^{F_n} \mathbf{SD}(i,j)} \quad (11)$$

where, F_n denotes the number of filters in the model. The process was repeated for all values of f , i.e., all 28 test frequencies. This specific procedure was implemented to emulate the effect of the traveling wave on the basilar membrane. Output of individual filters was assumed to be representative of neural (hair cell) stimulation and the scalar output representative of the contribution of all filters at a given frequency. The filter bank response was then assumed to be proportional to auditory sensitivity.

All values of ϕ_f were normalized from 0 to 1 to form the response curve of the humpback ear model. This function was compared to the predicted humpback whale audiogram described in Part 1. The absolute value of the maximum deviation between the ear model response curve and the predicted humpback audiogram across all tested frequencies was used as the performance metric (P_e) for tournament selection (Goldberg & Deb, 1991). Following sensitivity testing of all of the models in a generation, selection of parameter sets for inclusion in the next generation was determined via tournament selection with a tournament size of 10 (Goldberg & Deb, 1991).

EPs were run at the Navy High Performance Computing Center (SPAWARSYSCEN-San Diego) on a Hewlett-Packard V2500 multi-processor system. The V2500 utilized 16 440-MHz

4-way superscalar PA-8500 processors and 16 GB of RAM. Program code was multithreaded according to POSIX standards in order to take advantage of the HPC parallel processing capabilities (Norton & Dipasquale, 1997). Three EP simulations were performed with the predicted humpback sensitivity curve used as the target function. After each generation of a trial, the minimum P_e value produced by the current population of parameter sets was recorded. Trials were terminated if P_e decreased by less than 0.001 over a series of 100 generations.

Results

Predicting the humpback whale audiogram

The predicted humpback whale audiogram is presented in Figure 3. Sensitivity is plotted on a relative dB scale since there are no estimates of absolute auditory sensitivity for the humpback. The relative auditory sensitivity prediction for the humpback was U-shaped and typically mammalian. The region of best hearing, defined as relative sensitivity ≤ 0.2 , ranged from 700 Hz to 10 kHz, a range of almost 4 octaves. Maximum sensitivity, that which approached a value of zero, ranged from 2–6 kHz. Reduction in sensitivity was approximately 16 dB/octave above 10 kHz. Frequency sensitivity between 200–700 Hz was comparable to that between 10–14 kHz, both ranges covering relative sensitivities between 0.2 and 0.5, but with a shallower reduction in low frequency sensitivity of approximately 6 dB/octave. The most insensitive frequencies occurred at 100 Hz and frequencies ≥ 15 kHz.

Note that the broad range of frequencies to which humpbacks are predicted to be sensitive corresponds well to the range of frequencies reported for humpback whale sounds (Helweg *et al.*, 1998; Helweg *et al.*, 1990; Payne, 1983). Sound ranges are expected to reflect the same range of frequencies to which the whales would be sensitive.

Ear model performance

All ear filter models performed similarly. The best performing ear filter model had a $P_e=0.09$ (Figure 4b), a slightly better performance than the $P_e=0.10$ achieved by the other two models (Figure 4a and 4c). Two of the models converged upon configurations of 401 filters (Figure 4a and 4b) while the third utilized 263 filters (Figure 4c). Equations for determining filter Q_3 and the base value (y) of the amplitude scaling factor (S) were, respectively:

(Figure 4a)

$$Q_3=0.76*\exp((1.4e-2)*\mu)+0.34, y=2.92$$

(Figure 4b)

$$Q_3=0.69*\exp((1.5e-2)*\mu)+0.23, y=3.51$$

(Figure 4c)

$$Q_3=0.74*\exp((1.2e-2)*\mu)+0.69, y=2.06$$

Maximum deviations tended to occur above 5 kHz, though the 263-filter model configuration produced seven equivalent maximum deviations across the predicted range of hearing. Nevertheless, reduction in sensitivity above 10 kHz occurred at a rate similar to that predicted by the humpback audiogram. Frequencies of best sensitivity were at 3 and 5 kHz for all models and there was a consistent sensitivity roll-off below 700 Hz.

Discussion

In this study, a frequency-position function derived from the morphometry of the humpback whale basilar membrane (Ketten, in preparation) was combined with conventional land mammal psychoacoustic data and anatomical indices of hearing. As a result, the first audiogram for the humpback whale was predicted. This model provides a tool with which to aid mitigation of the acoustic exposure of humpback whales until such time that actual auditory sensitivities for these animals can be determined. Similar tools could be developed for other species of mysticete whale provided the anatomical data necessary for creating a frequency-position function are obtainable.

The ear models presented here are frequency spectrum filters or auditory weighting functions that allow a prediction of how the humpback auditory system attenuates sound according to frequency. It can be used to predict the magnitude of a frequency component of a received complex signal relative to that of other frequency components after filtration by the peripheral auditory system. Such predictions can improve the contextual interpretation of the response of mysticetes to sound exposure when the level of the signal received by the whale is known or can be estimated. These models only make use of frequency domain information and assume a static, but undefined, contribution of the outer and middle ear that is reflected in filter design. The model does not incorporate time domain characteristics or the dynamic contributions of the middle and outer ear. Advancement into more realistic lumped parameter models that account for additional mechanical properties of the auditory system is the next logical step. Such models provide a means of including the dynamic effects of middle and inner ear anatomy on system function and are more biologically relevant. Although these types of models have been applied to terrestrial mammals (Hubbard & Mountain,

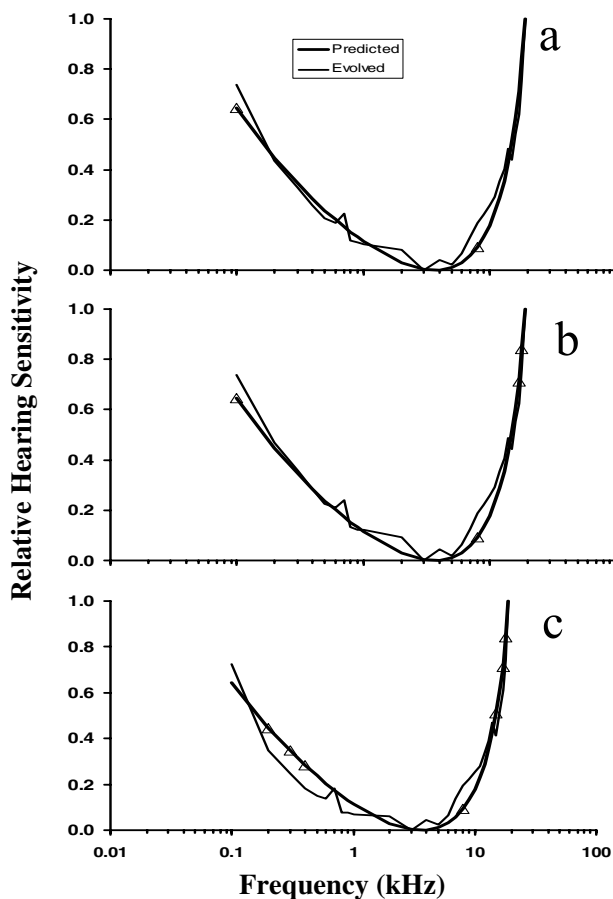


Figure 4. Comparison of the best-performing ear model output, from each evolutionary programming trial (panels a, b and c), to the predicted humpback relative sensitivity function. Triangles correspond to frequencies at which maximum deviations between the predicted humpback sensitivity function and model output occurred.

1996; Rosowski, 1996), their utility in modeling the auditory systems of marine mammals has yet to be realized.

Humpback whale songs span from near infrasonic frequencies to over 8 kHz (Helweg *et al.*, 1998; Helweg *et al.*, 1990; Payne, 1983). Predictions of hearing range reported here are in agreement with observed sound production for the humpback, which presumably lies within the range of hearing. Although the predicted audiogram demonstrates a plausible frequency-sensitivity shape, the zone of best sensitivity ($\sim 2\text{--}6$ kHz) is somewhat higher than one would predict after inspecting the distribution of frequencies used in humpback song. This is most likely explained by the contribution of the human and cat threshold functions to the predicted humpback whale audiogram. Although the use of

these values provided a generalized audiometric function for integration with the humpback whale basilar membrane frequency-position map, use of thresholds obtained from other mammals would undoubtedly cause some variation in the resulting U-shape. Thus, when implementing the humpback ear filter models, caution must be exercised when interpreting the results.

Methods of determining the impact of anthropogenic noise on mysticete whales will continue to rely heavily on the use of playback experiments and opportunistic observations of mysticete responses to the exposure of human-made sound. Models of mysticete hearing can augment these methods and should be pursued. The first bandpass filter models of the humpback whale ear are presented here to provide a means for contextually improving

interpretations of behavioral responses to sound exposure. These models should be used and built upon as more information about mysticete hearing becomes available and until such time that absolute auditory thresholds are experimentally determined.

Acknowledgments

This modeling effort was made possible by the estimates of humpback whale basilar membrane resonant frequencies generated by Dr. Darlene Ketten of the Woods Hole Oceanographic Institution, under contract from the Strategic Environmental Research and Development Program Project CS-1082. We thank the Space and Naval Warfare Systems Center High Performance Computer Center for their grant of CPU time on the HP V2500. This study was possible in part thanks to funds from PMS-400DE and SERDP Project CS-1082. The procedures involved in this study comply with the 'Principles of Animal Care', publication No. 86-23 (revised 1985), of the National Institute of Health and with the current laws of the United States of America.

Literature Cited

- Au, W. W. L. (1993). *The Sonar of Dolphins*. Springer-Verlag; New York.
- Au, W. W. L. & Moore, P. W. B. (1990). Critical ratio and critical bandwidth for the Atlantic bottlenosed dolphin. *J. Acoust. Soc. Amer.* **88**, 1635–1638.
- Busnel, R.-G. & Fish, J. (1979). *Animal Sonar Systems*. In: NATO ASI, vol. 28. Plenum; New York, pp. 1135.
- Chellapilla, K. & Fogel, D. B. (1997). Two new mutation operators for enhanced search and optimization in evolutionary programming. In: *SPIE's International Symposium on Optical Science, Engineering, and Instrumentation*, Conference 3165: Applications of Soft Computing. SPIE Press, pp. 260–269.
- Clark, C. W. (1990). Acoustic behavior of mysticete whales. In: J. Thomas and R. Kastelein, (eds.) *Sensory Abilities of Cetaceans*, vol. 196. NATO ASI Series Plenum Press; New York, pp. 571–583.
- Fay, R. R. (1988). *Hearing in Vertebrates: A Psychophysics Handbook*. Hill-Fay Associates; Winnetka, Illinois.
- Fogel, D. B. (1995). *Evolutionary Computation: Toward a New Philosophy of Machine Learning*. IEEE Press; Piscataway, NJ.
- Frankel, A. S. & Clark, C. W. (1998). Results of low-frequency playback of M-sequence noise to humpback whales, *Megaptera novaeangliae*, in Hawai'i. *Can. J. Zool.* **76**, 521–535.
- Geisler, D. C. & Cai, Y. (1996). Relationships between frequency-tuning and spatial-tuning curves in the mammalian cochlea. *J. Acoust. Soc. Amer.* **99**, 1550–1555.
- Goldberg, D. E. & Deb, K. (1991). A comparative analysis of selection schemes used in genetic algorithms. In: (G. Rawlins, ed) *Foundations of Genetic Algorithms*. Morgan Kaufman; San Mateo, pp. 69–93.
- Greenwood, D. D. (1990). A cochlear frequency-position function for several species - 29 years later. *J. Acoust. Soc. Amer.* **87**, 2592–2605.
- Helweg, D. A., Cato, D. H., Jenkins, P. F., Garrigue, C. & McCauley, R. D. (1998). Geographic variation in South Pacific humpback whale songs. *Behaviour* **135**, 1–27.
- Helweg, D. A., Herman, L. M., Yamamoto, S. & Forestell, P. H. (1990). Comparison of songs of the humpback whales (*Megaptera novaeangliae*) recorded in Japan, Hawaii, and Mexico during the winter of 1989. *Sci. Rep. Cetacean Res.* **1**, 1–20.
- Herman, L. M. & Arbeit, W. R. (1972). Frequency difference limens in the bottlenose dolphin: 1–70 KC/S. *J. Aud. Res.* **2**, 109–120.
- Herman, L. M. & Tavolga, W. N. (1980). The communication systems of cetaceans. In: L. M. Herman, (ed.) *Cetacean Behaviour* Wiley Interscience; New York, pp. 149–209.
- Houser, D. S., Helweg, D. A., Chellapilla, K. & Moore, P. W. (2001). Optimizing alternative models of dolphin auditory sensitivity using evolutionary computation. *Bioacoustics* **In Press**.
- Hubbard, A. E. & Mountain, D. C. (1996). Analysis and synthesis of cochlear mechanical function using models. In: H. L. Hawkins, T. A. McMullen, A. N. Popper and R. R. Fay, (eds.) *Auditory Computation*, vol. 8. Springer Handbook of Auditory Research. Springer; New York, pp. 62–120.
- Johnson, C. S. (1968a). Masked tonal thresholds in the bottlenosed porpoise. *J. Acoust. Soc. Amer.* **44**, 965–967.
- Johnson, C. S. (1968b). Relation between absolute threshold and duration-of-tone pulses in the bottlenosed porpoise. *J. Acoust. Soc. Amer.* **43**, 757–763.
- Ketten, D. R. (1993). Low frequency tuning in marine mammal ears, Symposium on Low Frequency Sound in the Ocean. In: Tenth Biennial Conference on the Biology of Marine Mammals, pp. 3.
- Ketten, D. R. (1994). Functional analysis of whale ears: Adaptations for underwater hearing. In: *Proceedings in Underwater Acoustics*, vol. 1, p. I-264-I-270.
- Ketten, D. R. (1997). Structure and function of whale ears. *Bioacoustics* **8**, 103–135.
- Ketten, D. R. & Wartzok, D. (1990). Three-dimensional reconstruction of the dolphin cochlea. In: J. A. Thomas and R. A. Kastelein, (eds.) *Sensory Abilities of Cetaceans: Laboratory and field Evidence* Plenum Press; New York, pp. 81–105.
- Lieberman, C. M. (1982). The cochlear frequency map for the cat: Labeling auditory-nerve fibers of known characteristic frequency. *J. Acoust. Soc. Amer.* **72**, 1441–1449.
- Malme, C. I., Miles, P. R., Tyack, P. L., W., C. C. & E., B. J. (1985). Investigation of the potential effects of underwater noise from petroleum industry activities on feeding humpback whale behavior. Bolt, Beranck, and Newman Laboratories; Cambridge, MA.
- Malme, C. I., Würsig, B., Bird, J. E. & Tyack, P. (1988). Observations of feeding gray whale responses to controlled industrial noise exposure. In: W. M. Sackinger, M. O. Jeffries, J. L. Imm and S. D. Tracey, (eds.) *Port and Ocean Engineering Under Arctic Conditions*, vol. 2. Geophysical Institute, University of Alaska; Fairbanks, AK, pp. 55–73.

- Maybaum, H. L. (1989). Effects of 3.3 kHz sonar system on humpback whales, *Megaptera novaeangliae*, in Hawaiian waters. *Eos* **71**, 92.
- Nachtigall, P. E. & Moore, P. W. B. (1988). *Animal Sonar: Processes and Performance*. In NATO ASI, vol. 156. Plenum Press; New York, pp. 862.
- Norris, J. C. (1981) *Auditory Morphology in Whales and Dolphins*. Master's Thesis; University of California, San Diego, CA.
- Norton, S. J. & Dipasquale, M. D. (1997). *Threadtime: Multithreaded Programming Guide*. Prentice Hall PTR; Upper Saddle River, NJ.
- Payne, R. S. (1983). Communication and behavior of whales. In: *AAAS Selected Symposium Series*. Westview Press; Boulder, CO, pp. 643.
- Popov, V. V., Supin, A. Ya. & Klishin, V. O. (1996). Frequency tuning curves of the dolphin's hearing: envelope-following response study. *J. Comp. Physiol. A* **178**, 571–578.
- Popov, V. V., Supin, A. Ya. & Klishin, V. O. (1997). Frequency tuning of the dolphin's hearing as revealed by auditory brain-stem response with notch-noise masking. *J. Acoust. Soc. Amer.* **102**, 3795–3801.
- Richardson, J. W., Würsig, B. & Greene, C. R., Jr. (1990). Reactions of bowhead whales, *Balaena mysticetus*, to drilling and dredging noise in the Canadian Sea. *Mar. Environ. Res.* **29**, 135–160.
- Richardson, W. J., Fraker, M. A., Würsig, B. & Wells, R. S. (1985). Behaviour of bowhead whales *Balaena mysticetus* summering in the Beaufort Sea: Reactions to industrial activities. *Biol. Conserv.* **32**, 195–230.
- Richardson, W. J. & Würsig, B. (1997). Influences of man-made noise and other human actions on cetacean behaviour. *Mar. Fresh. Behav. Physiol.* **29**, 183–209.
- Roitblat, H. L., Moore, P. W. B., Helweg, D. A. & Nachtigall, P. E. (1993). Representation of acoustic information in a biomimetic neural network. In: J. A. Meyer, S. W. Wilson and H. L. Roitblat, (eds.) *From Animals to Animats 2: Simulation of Adaptive Behavior* MIT Press; Cambridge, MA, pp. 90–99.
- Rosowski, J. J. (1996). Models of external- and middle-ear function. In: H. L. Hawkins, T. A. McMullen, A. N. Popper and R. R. Fay, (eds.) *Auditory Computation*, vol. 8. Springer Handbook of Auditory Research. Springer; New York, pp. 15–61.
- Schwefel, H.-P. (1981). *Numerical Optimization of Computer Models*. Wiley; New York.
- Supin, A. Ya., Popov, V. V. & Klishin, V. O. (1993). ABR frequency tuning curves in dolphins. *J. Comp. Physiol. A* **173**, 649–656.